Polymer Degradation and Stability 247 (2026) 111981

Contents lists available at ScienceDirect

Polymer Degradation and Stability

journal homepage: www.journals.elsevier.com/polymer-degradation-and-stability

Polymerization catalyst is key: Predicting molecular changes during mechanical recycling of phillips and ziegler-natta catalyst high-density polyethylene (HDPE)

Alexsandar Arumugam [a], Jana Zimmermann [b], Thea Weingartz [a], Michael Fischlschweiger [b], Valerian Hirschberg [a,*]

[a] Institute of Technical Chemistry, Clausthal University of Technology, Germany
[b] Institute of Energy Process Engineering and Fuel Technology, Clausthal University of Technology, Germany

ARTICLE INFO

Key words:
High-density polyethylene (HDPE)
Phillips and Ziegler-Natta catalyst
Recycling
Rheological characterization
Extensional rheology
Catalyst-specific degradation
Strain hardening

ABSTRACT

We present a systematic approach to predict the molecular degradation of high-density polyethylene (HDPE) during mechanical recycling based on the polymerization catalyst. HDPE represents about 12.5 wt % of the polymer world production and is industrially mainly produced by Phillips (P-HDPE) and Ziegler-Natta catalyst (ZN-HDPE). Two blow-moulding P- and ZN—HDPE with identical melt flow indices (MFI) were subjected to mechanical recycling at an extrusion temperature of 170 °C and 210 °C, a screw speed of 180 rpm, and recycling times from 10 to 240 min. Chemical and rheological characterization revealed, that despite similar initial melt properties, P-HDPE and ZN- HDPE exhibited fully contrary degradation mechanisms: for recycled P- HDPE at 170 °C and 210 °C, the complex viscosity ($|\eta^*|$) and the molecular weight drastically increased after 10 min of recycling time due to star-like branching, followed by chain scission at 170 °C, but crosslinking at 210 °C, resulting in unprocessable, rubber-like material. In contrast, recycled ZN—HDPE exhibited a continuous drop in molecular weight and in $|\eta^*|$ across all conditions. This work provides a polymerization catalyst-specific framework to predict and engineer thermo-mechanical molecular degradation pathways in HDPE recyclates, paving the way to tailored recycling strategies to obtain value-added materials.

1. Introduction

The global consumption of plastics continues to increase at an unprecedented rate, with packaging applications alone accounting for a substantial proportion of this demand [1]. High density polyethylene (HDPE) is one of the most widely used polymers in packaging, owing to its high strength, chemical resistance, and cost-effectiveness [2]. In 2024, the global production of plastics reached 418 million tonnes (Mt), [3]. of which HDPE constituted approximately 52.6 Mt, accounting for ~12.5 % of total output. Notably, packaging represented the predominant end-use sector for HDPE, with >60 % of global HDPE production directed toward packaging applications [4]. However, the short lifespan of packaging application, often less than one year, [1]. contributes significantly to plastic waste, creating considerable environmental concerns.

Mechanical recycling has emerged as a promising solution for reprocessing plastic waste, due to its straight forward reuse of the material. However, due to the applied high temperatures and mechanical stresses acting on the polymer, mechanical recycling can lead to molecular degradation phenomena such as chain scission, branching, or crosslinking. Generally, the degradation behaviour of a polymer and its structural changes during mechanical recycling depends mainly on the repeating unit (monomer) and its functional groups, M_w, the polymer architecture, and catalyst used during polymerization [5–7]. Molecular degradation significantly alters the viscoelastic melt flow behaviour, quantified in first approximation by melt flow index (MFI) but also with high sensitivity by shear and extensional rheological measurements [8]. An overview about previous literature on mechanical recycling of HDPE is given in the Table 1. It is striking that some authors observe independent of the recycling conditions M_w increase due to branching or crosslinking after recycling and others observe a decrease in M_w due to chain scission. This is marked in Table 1 by the green and red arrows up and down.

The molecular topological changes are intricately reflected in the

* Corresponding author.
E-mail address: valerian.hirschberg@tu-clausthal.de (V. Hirschberg).

https://doi.org/10.1016/j.polymdegradstab.2026.111981
Received 4 December 2025; Received in revised form 27 January 2026; Accepted 2 February 2026
Available online 3 February 2026

material's viscoelastic relaxation behaviour, which rheology quantifies with high sensitivity [18–20]. Properties extracted from small amplitude oscillatory shear (SAOS) data, [19]. such as zero-shear viscosity (η_0) or crossover frequency (ω_{co}) of storage and loss modulus (G' and G'') or strain hardening in extensional flow are direct indicators of changes in M_w and molecular topology, such as branching, of a polymer [21]. Especially strain hardening in extensional flow plays a pivotal role in evaluating melt strength and is a key requirement for advanced and high value polymer processing operations such as film blowing, [22]. fibre spinning, [23]. foam extrusion, [24]. and thermoforming, [25]. where the polymer is subjected to uniaxial or biaxial stretching. For PE, strain hardening is caused on the molecular level typically by long-chain branching [26]. (LCB), thus its presence or absence leaves a clear topological fingerprint. Therefore, rheological characterization especially when combining the molecular information obtained from shear and extensional flows is indispensable for understanding and predicting degradation pathways and to develop material upcycling strategies.

The shear rheology of linear polymer chains is governed by reptation theory and for strain rates below the inverse Rouse relaxation time, they typically do not show strain hardening in uniaxial extensional flow [27,28]. Star-like branching (see Fig. 1) leads to higher η_0 compared with a linear polymer, as for symmetric stars η_0 scales exponentially with the arm molecular weight. However, in extensional flow stars also do not show strain hardening, due to the absence of a second branching point within the molecule to induce chain stretch [29,30]. As shown in literature for branched pom-pom model systems with arms exceeding three entanglements in molecular weight and being longer than the backbone can behave like stars [29,31,32]. In this case the relaxation time of the arms governs the relaxation behaviour of the full molecule [29]. In contrast, long-chain branched topologies (see Fig. 2), i.e., where the molecular weight of the backbone is significantly higher than the molecular weight of the arms, show strong shear thinning and strain hardening due to chain stretch between the branching points in extensional flow. Consequently, rheology is a highly powerful tool to probe molecular dynamics and correlate them with molecular topology [28,33].

HDPE is industrially mainly produced using a Phillips [34], Ziegler-Natta [35–37]. and metallocene [38]. type catalyst system. About 80 wt % of HDPE is manufacturing from chromium (Cr) based Phillips [34]. and titanium (Ti) based Ziegler-Natta catalysts [28]. P-HDPE typically contains terminal vinyl groups, whereas ZN—HDPE has only few unsaturated carbon-carbon [29,32,33].

The objective of this work is to systematically examine the mechanical recycling behaviour and the molecular degradation pathways of two HDPE with similar viscoelastic melt properties but synthesized with different polymerization catalyst, namely a P-HDPE and a ZN—HDPE (Fig. 2). Both are blow moulding grade samples with similar MFI and relatively similar M_w. A twin-screw extruder is used at two processing temperatures of 170 °C and 210 °C, different residence times from 10 to 240 min, and a screw speed of 180 rpm to simulate mechanical recycling. The MFI, differential scanning calorimetry (DSC), cross-fractionation chromatography (CFC), rheological SAOS and extensional rheological measurements were used to characterize molecular degradation. The findings offer a molecular-level understanding of how polymerization catalyst type influences the molecular degradation mechanisms and rheological properties, with direct implications for recycling conditions that pave the way to functional recovery and upcycling of HDPE waste streams.

2. Materials and methods

2.1. Raw materials

Two blow-moulding grade HDPE were used in this study, virgin vZN—HDPE (Borstar BB4588) supplied by Borealis, and virgin vP-HDPE (Lupolen 5012DX) sourced from LyondellBasell. Both materials exhibited comparable MFI of 0.23 and 0.25 g/10 min, respectively, measured at 190 °C under 2.16 kg load, following ASTM D 1238.

Both HDPE have relatively similar M_w, but differ largely in dispersity, have quasi-identical melting temperatures of 133 °C, but different degrees of crystallinity, which are given in Table 2. Chemical characterization of the two virgin HDPEs was performed using Fourier-transform infrared (FTIR) spectroscopy and high-temperature size exclusion chromatography (HT-SEC) from CFC, as presented in Fig. 3. While both materials exhibit overall similar chemical structures, the FTIR spectra reveal a subtle but distinct absorption band near 908 cm^{-1} only in the vP-HDPE sample.

This band is characteristic of terminal vinyl groups (–CH═CH₂), suggesting the presence of unsaturated end groups in the vP-HDPE. Such chemical features have been previously reported in the literature for HDPE produced via Phillips-type catalysis [39–41]. HT-SEC analysis (Fig. 3) indicates that this vZN-HDPE possess a much broader, trimodal

Table 1
Previous research on HDPE mechanical recycling and its rheological observation. The contradicting findings regarding Mw increase or decrease are marked with green and red arrows, pointing up or down.

Author	Type of extruder	Extrusion screw speed and Temperature	Recycling time/ Number of recycling cycle	HDPE supplier details	Observation	Change in M_w
Zhang et al. [9, 10]	Co-rotating twin screw extruder	60 rpm, 170 °C	Up to 16 cycles, 1 cycle = 90 s	M_w = 94.5 kg/mol, MFI = 6.7 g/10 min, T_m = 132 °C	No changes cycle 0 to 4. 4–8 cycles: increase in η_0 due to star-like branching. M_w in SEC reduced by 11 % up to 16th cycle.	↑
Oblak et al. [11]	Co-rotating twin screw extruder	150 rpm, 240 °C	0 to 100 cycles	LANUFENE HDI-6507UV, MFI = 7.5 g/10 min	MFI decreases from 7.5 to 0.096 g/10 min for cycle 0 to 100. Complex viscosity increases with increased number of cycles.	↑
Zahavich et al. [12]	Single screw extruder	80 rpm, 215 °C	Up to 4 cycles, 1 cycle = 2 min	homo- and copolymer MFI = 0.32 and 0.79 g/10 min	MFI decreases. Viscosity increases from cycle 0 to 4, while crossover frequency decreases, indicating crosslinking.	↑
Schülein et al. [13]	Closed cavity rheometer	$\omega/2\pi$ = 1, Hz γ_o = 27 % to 460 %, 220 °C	Up to 300 min	MFI = 0.25 g/10 min, M_w = 113.2 kg/mol	Molecular weight increases due to branching and maximum SHF is 2.7.	↑
Teteris et al. [14]	Single screw extruder	20 rpm, 230 °C	up to 5 cycles	MFI = 1.4 g/10 min	MFI and crystallinity increase from cycle 0 to 5	↓
Benoit et al. [15]	Co-rotating twin screw extruder	125 rpm, 200 °C	up to 50 cycles	MFI = 0.2 g/10 min, M_w =157 g/mol, 44 % crystallinity	MFI increases from 0.2 g/10 min to 0.5 g/10 min from recycling cycles 0 to 50 due to chain scission.	↓
Schweighuber et al. [16]	Twin screw extruder	50 rpm, 100 rpm, 220 °C	up to 120 min	powder from local manufacturer	M_w decreases, quantified via HT-SEC-IR.	↓
Andersson et al. [17]	Single screw extruder with online rheometer	100 rpm, 260 °C to 325 °C		MFI = 9 g/10 min, $Đ$ = 14	Viscosity decreases at both temperatures, chain scission.	↓

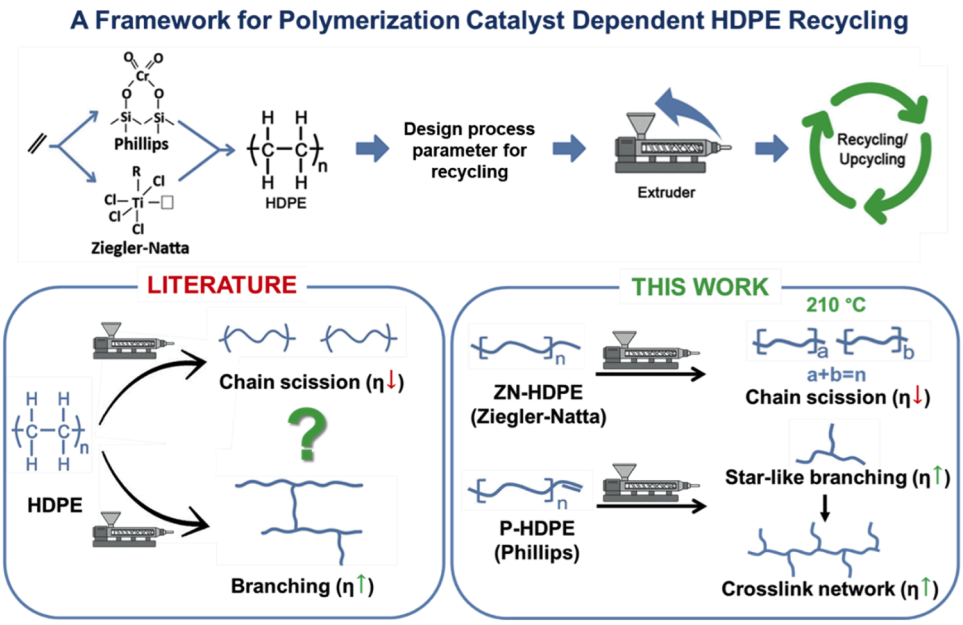

Fig. 1. Path-dependent rheological evolution of HDPE during thermal–mechanical recycling: Toward rational upcycling design.

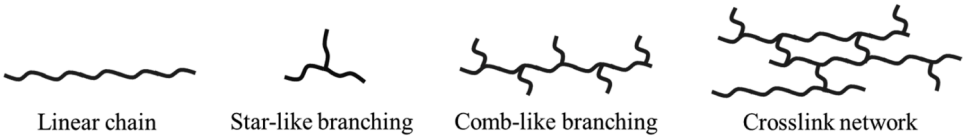

Fig. 2. Different architypes topologies of polymers: linear polymer, star-like and comb-like long-chain branching (LCB) as well as a chemically crosslinked polymer network.

Table 2
Material and molecular information such as grade name, M_w, Đ, MFI, T_m and degree of crystallinity, X_c, of the virgin raw materials.

Raw material	Grade Name	M_w [kg/mol]	Đ	MFI [2.16 kg and 190 °C]	T_m [°C]	X_c [%]
vP-HDPE	Lupolen 5012DX, Lyondell Basell	232	20	0.25 g/10 min	133 °C	66.6
vZN-HDPE	Borstar BB2588, Borealis	273	42	0.23 g/10 min	133 °C	72.4

molecular weight distribution (MWD) compared to a monomodal MWD for the vP-HDPE.

2.2. Mechanical recycling method

Mechanical recycling experiments were performed using a Haake Minilab II co-rotating twin screw extruder via the circulation mode, where the material continuously flows within the barrel. HDPE samples were processed at two fixed temperatures (T_r), 170 °C and 210 °C, a screw speed of 180 rpm and recycling time (t_r) in the extruder of 10, 20, 30, 60, 120, and 240 min. Each processing condition was applied to both HDPE types to evaluate the impact of reprocessing on thermal and rheological properties. After the extrusion, recycled materials were subjected to chemical characterization such as FTIR, DSC and CFC and rheological measurements like SAOS and extensional rheology. The specimen for rheology were produced by compression moulding in a melt press at 180 °C under vacuum, with disks of 25 mm diameter and 1 mm thickness for the SAOS measurement and rectangular specimen with dimension of 15 mm length, 5 mm width and 0.5 mm thickness for extensional rheology.

2.3. Melt flow index (MFI)

MFI was conducted with device from Custom scientific instruments (CSI) according to the ASTM D1238 at 190 °C and 2.16 kg load. MFI values were calculated by weight (in unit g) of samples extrudate in 10 min.

2.4. Differential scanning calorimetry (DSC)

Thermal analysis was performed using a DSC by Mettler Toledo 1 from the temperature of -80 °C to 180 °C with heating and cooling rate of 10 K/min. The percentage of crystallinity and the melting temperature was calculated in the second cooling and heating cycle. The percentage of crystallinity (X_c), is calculated as shown in Eq. (1) with $\Delta H_{m100} = 293$ J/g [42].

$$Xc = \frac{\Delta H_m}{\Delta H_{m100}} \cdot 100\ \% \quad (1)$$

2.5. Rheology

SAOS rheological measurements were carried out on an Anton Paar rotational rheometer (MCR 702e Space, Austria) with parallel plate (25 mm diameter and 1 mm thickness) under N_2 inert gas atmosphere (N_2 5.0, 99.999 % N_2 purity). Initially, a strain sweep test was done at 160 °C with a constant frequency of 100 rad/s to obtain the viscoelastic linear regime, where G' and G'' are constant as a function of strain amplitude. Frequency sweep tests are performed at 160 °C and a frequency range of 150 to 0.001 rad/s and a constant strain amplitude in the linear viscosity regime. Extensional rheological measurements were performed at 160

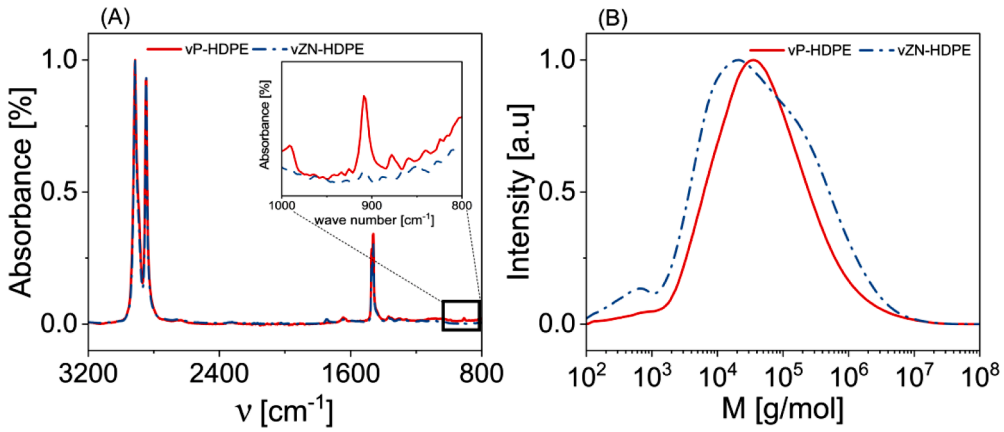

Fig. 3. (A): FTIR spectra of vP-HDPE and vZN—HDPE, highlighting characteristic absorbance bands. The presence of terminal vinyl unsaturation in vP-HDPE is indicated by distinct peaks around 908 cm^{-1} which is absent or significantly reduced in vZN—HDPE compared to vP-HDPE. (B) SEC traces of vP-HDPE and vZN—HDPE, illustrating differences in molecular weight distribution.

°C at different Hencky strain rates (3 s^{-1}, 1 s^{-1}, 0.3 s^{-1}, 0.1 s^{-1} and 0.03 s^{-1}) by using the universal extensional fixture (UXF) from Anton Paar in the multidrive mode. The strain hardening factor (SHF), defined as the ratio of the transient extensional viscosity to the steady state viscosity of the Doi-Edwards model, [43,44]. calculated via the IRIS software [45]. was used to quantify the strain hardening behaviour of virgin and recycled HDPEs under uniaxial extension at different strain rates.

2.6. Cross-Fractionation chromatography (CFC)

CFC analysis was done by temperature rising elution fractionation (TREF) and SEC from Polymer Char. Initially 8 mg sample was dissolved in 1,2,4-trichlorobenzene at 150 °C for 60 min. This solution is injected to the TREF column filled with ceramic-micro balls of a void volume of 2000 to 2600 μL first, followed by a SEC column (PLgel Olexis, 7.5 × 300 mm, 13 μm pore size). The temperature of the TREF column starts to drop with a rate of 0.5 °C min^{-1} from 125 °C to 35 °C to let the polymer crystallize out of the solution almost under equilibrium conditions, to avoid co-crystallization. Followed by the elution enters the SEC for molar weight distribution analysis.

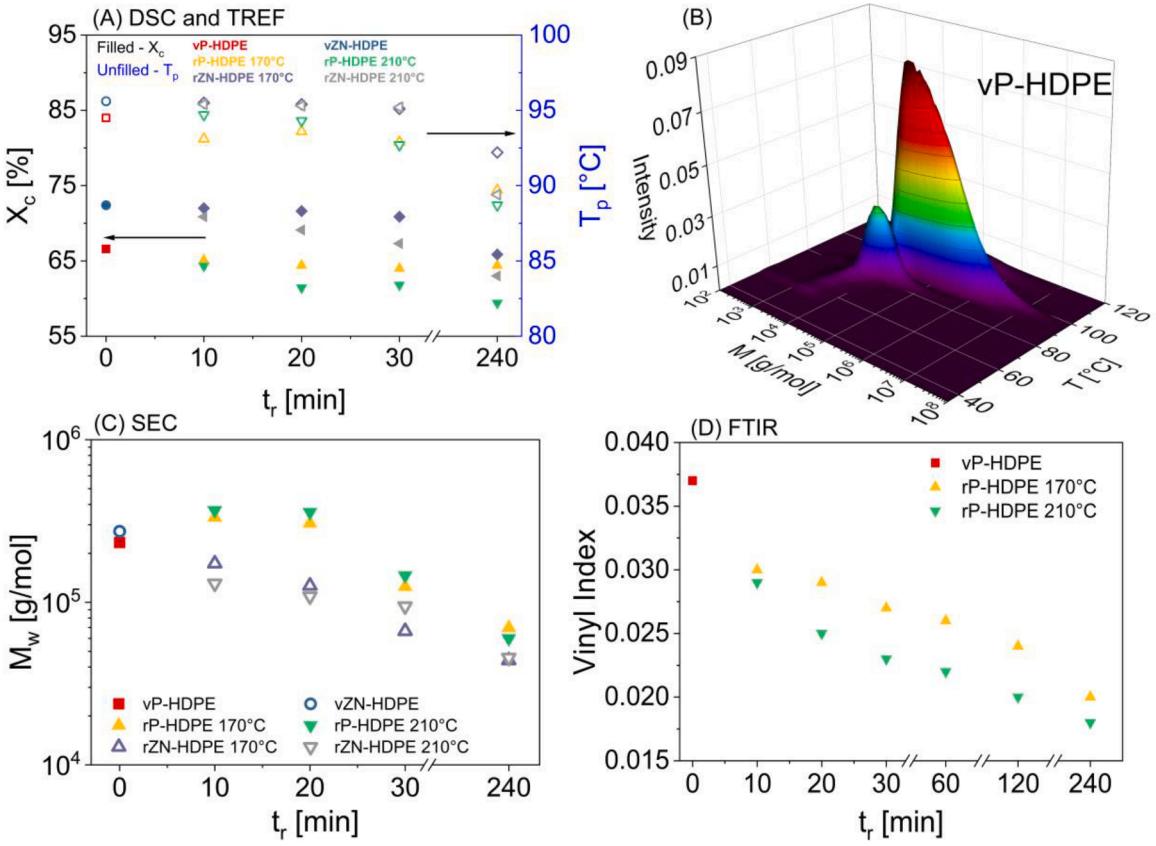

Fig. 4. (A) shows crystallinity from DSC and peak temperature in TREF of the recycled samples as a function of recycling time, (B) is a 3D plot of CFC analysis of vP-HDPE, and (C) shows M_w of rP- and rZN—HDPE recycled at 10, 20, 30 and 240 min from SEC-IR and (D) is vinyl index of recycled P—HDPE from FTIR analysis.

2.7. Fourier-transform infrared (FTIR) spectroscopy

FTIR spectroscopy was conducted using a BRUKER Alpha-T spectrometer over the wavenumber range of 3600 to 600 cm^{-1} at room temperature. The measurements were acquired with a spectral resolution of 4 cm^{-1}, averaging 256 scans per sample. The vinyl index (VI) is calculated by using Eq. (2) [46].

$$Vinyl\ Index = \frac{A_{908cm^{-1}}}{A_{1465cm^{-1}}} \quad (2)$$

3. Result and discussions

3.1. Differential scanning calorimetry

DSC was employed to investigate the thermal behaviour of virgin and recycled HDPE samples, to quantifying the impact of the recycling-induced molecular degradation on melting temperature (T_m) and degree of crystallinity (X_c). The changes in X_c are shown in Fig. 4(A). The raw data of heat flow vs temperature can be found in the SI (Figure S1 and Table S1). vP-HDPE and vZN-HDPE showed X_c values of 66.6 % and 72.4 %, respectively. For P—HDPE, X_c decreased continuously with increasing t_r at both T_r, with a stronger decrease at $T_r = 210$ °C to 59.4 % after $t_r = 240$ min, reflecting increased topological irregularities like branching and more topological irregularities at higher T_r that disrupt crystalline packing. The same trend was observed in rZN-HDPE, recycling at both T_r led to a reduction in crystallinity, with X_c decreased to 66 % after 240 min at $T_r = 170$ °C, whereas at $T_r = 210$ °C, X_c decreased to 63 % at $t_r = 240$ min. The overall reduction in crystallinity for both materials is primarily attributed to the formation of irregularities within the polymer chain, such as short- and long-chain branching. vP-HDPE and vZN—HDPE exhibited melting temperatures (T_m) of about 133.0 °C. Upon recycling, T_m progressively decreased with increasing t_r and T_r, primarily due to the formation of branches during thermal-mechanical degradation. For rP-HDPE, T_m decreased at $T_r = 170$ °C, to 128.5 °C after the $t_r = 240$ min, and at $T_r = 210$ °C, T_m declined to 129.2 °C at $t_r = 240$ min. A similar trend was observed for rZN—HDPE, with T_m decreased to 129.8 °C ($t_r = 40$ min) at $T_r = 170$ °C and at $T_r = 210$ °C, T_m decreased to 126.7 °C when $t_r = 240$ min. The decrease in T_m of rP-HDPE and rZN—HDPE clearly indicates that branches are formed during the recycling process.

3.2. Chemical characterization

CFC is coupling of SEC with TREF, was employed to investigate the formation of chain irregularities such as branching, mainly short-chain branching (SCB), [47–49]. in correlation with M_w of P-HDPE and ZN—HDPE during recycling (Figure S2 and Table S2).

The vP-HDPE exhibited a relatively narrow molecular weight distribution ($M_w = 232$ kg/mol, $Đ = 20$), moderate crystallinity from DSC of $X_c = 66.6$ %, a value of 3.8 for CH_3/1000 total carbon atoms (TC) and a TREF peak temperature (T_p) of 94.5 °C. The T_p in TREF reflects the crystallizability of a polymer fraction, governed by its average branching content [50–52]. Higher T_p indicate more linear, crystalline segments, while lower T_p correspond to more branched, less crystalline fractions. Recycling of P-HDPE at shorter $t_r = 10$ min at both T_r lead to only small changes in T_p, whereas the parameter CH_3/1000 TC from 3.8 for vP—HDPE significantly decreased to 2.5 and 2.9 at 170 °C and 210 °C respectively, which indicates reduction in the chain ends. The value of CH_3/1000 drastically increased above the value of the vP-HDPE up to a factor of 3 by increased t_r from 30 to 240 min. Additionally, SEC shows for P-HDPE at both T_r an increase in M_w after $t_r = 10$ min due to the branching or crosslinking. Starting with $t_r = 30$ min, M_w decreases, reaching at $t_r = 240$ min for both temperatures a M_w decrease of nearly 70 %. However, the elution volume is measured against a linear PS standard, thus long-chain branching is not represented properly.

In contrast, vZN-HDPE showed higher crystallinity of $X_c = 72.4$ %, higher M_w and broader molecular weight distribution (M_w is 273 kg/mol, $Đ = 42$), and slightly larger CH_3/1000 TC of 4.8, with a higher T_p of 95.6 °C. As shown by SEC, recycling of ZN—HDPE led to a continuous drop in the observed molecular weight. At $T_r = 170$ °C, M_w decreased to $M_w = 173$ kg/mol after $t_r = 10$ min and $M_w = 44$ kg/mol about $t_r = 240$ min, with a reduction of dispersity to about 70 %. The change in dispersity shows, that particularly the long polymer chains undergo chain scission. At $T_r = 210$ °C, M_w is reduced to $M_w = 130$ kg/mol after $t_r = 10$ min and to $M_w = 45$ kg/mol after $t_r = 240$ min. From TREF, T_p does not change after $t_r = 30$ min for both T_r, however decreases slightly at $t_r = 240$ min, indicating simply chain scission but no (significant) branching at $t_r = 30$ min. This is in line with the small changes in the parameter CH_3/1000 TC, at both T_r, whereas at $t_r = 240$ min the content of chain ends doubles. Overall, CFC analysis reveals that recycling of P—HDPE initially caused chain extension and M_w increase, but prolonged t_r led to severe apparent M_w reduction and extensive branching. In contrast, ZN—HDPE primarily underwent chain scission, with M_w and dispersity decreasing while branching increased only at longer t_r. These findings highlight the catalyst-dependent structural stability of HDPE under recycling conditions.

A difference in branching mechanism can be observed also from IR spectroscopy: vP-HDPE exhibited a terminal vinyl group, with a ratio of 0.037 per 1000 carbon atoms, consistent with chain-end unsaturation generated during polymerization. During recycling, a progressive decrease in vinyl content as a function of t_r was observed, as shown in Fig. 4D, with a more pronounced decrease at higher T_r. At 170 °C and 210 °C, the vinyl concentration decreased after $t_r = 10$ min by 19 % and 22 % and after $t_r = 240$ min by 45 % and 52 %, respectively. The terminal vinyl bonds disappear due to a chemical reaction, suggesting e.g., a crosslinking of two or more terminal double bonds, leading to higher molecular weight structures. The systematic decline in vinyl content with increasing t_r thus provides a molecular-level indicator of topological changes occurring during the thermal-mechanical degradation of rP-HDPE, with a faster reaction speed/faster disappearing of the terminal double bonds at higher temperatures. In contrast, vZN—HDPE does not show any significant vinyl index with an absence of the peak at 908 cm^{-1}, as shown in Fig. 3.

3.3. Melt flow index

The MFI quantifies how easily the polymer melt flows under specific conditions, and it is an important measure in polymer processing industries. Processing temperature and recycling time significantly

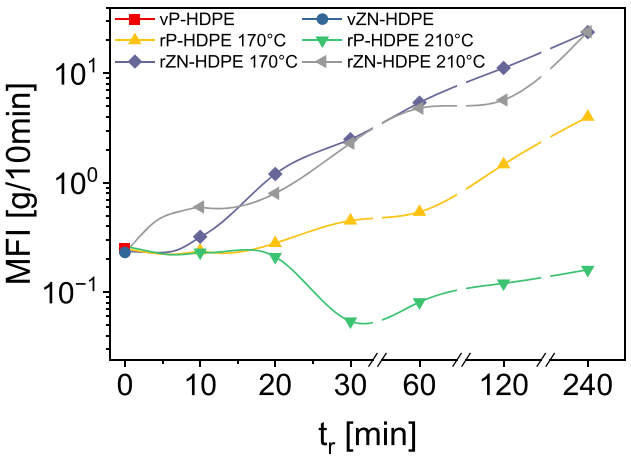

Fig. 5. MFI as a function of recycling time at different temperatures for virgin and recycled P-HDPE and ZN—HDPE.

influence the MFI of rP-HDPE and rZN—HDPE. As shown in Fig. 5 and Table S3, vP-HDPE and vZN—HDPE exhibited MFI values of 0.25 and 0.23 g/10 min, respectively. Mechanical recycling of P-HDPE did result in a slight decrease after 10 and 20 min at both temperatures, before at after 30 min of recycling time the material behaviour clearly differs: At 170 °C, the MFI rapidly increases and doubles compared to its original value after 30 min and a drastic increase by a factor of 16 after 240 min. In contrast, at T_r = 210 °C, the MFI decreased by a factor of 5 to a basically crosslinked, thus very high viscosity material.

For ZN—HDPE at 170 °C and 210 °C a continius increase in MFI was observed, associated with molecular weight reduction. After 30 min, the MFI increased by a factor of 10 and 11 to around 2.5 g/10 min and 2.55 g/10 min, respectively, with similar MFI values as an injection moulding grade. After 240 min, the MFI increase for both recycling temperature by more than a factor of 100. Those trends strongly suggest different degradation pathways (see below) for rP-HDPE and rZN-HDPE and that higher temperatures promote crosslinking or branching in rP—HDPE and chain scission in rZN-HDPE.

3.4. Small amplitude oscillatory shear (SAOS) rheology

The rheological behaviour of virgin and recycled HDPEs was investigated using rheological SAOS measurements and analysing the SAOS G' and G'' vs ω (Fig. 6 and Figure S3) and |η*| vs ω data (Fig. 6C). Molecular changes were quantified via the crossover frequency (ω_{co}) from the rubber to the terminal regime defined as the angular frequency at which storage (G') and loss (G'') moduli intersect ($G' = G''$) and via |η*| at a low frequency of 0.01 rad/s (Table S4, Figure S4). Both parameters are sensitive to molecular weight and chain dynamics, thus allow to investigate the degradation mechanism.

For P—HDPE, Fig. 6(B) shows, that ω_{co} decreases after t_r = 10 min at T_r = 170 °C, by a factor of 25 and for T_r = 210 °C by a factor of 100, indicating very sensitively massive M_w increase or the formation of a (dominating) star-like topology with a very large longest relaxation time [53]. For a linear polymer, a decrease of ω_{co} by a factor of 25 or rather 100 corresponds to a M_w increase by a factor of 2.6 and 3.9, following reptation theory and $M_w \propto 1/\omega_{co}^{3.4}$, [21,54]. Since SEC shows only a M_w increase of only 40 % and 58 %, this hints to the formation of branched, star-like topologies, where the crossover-frequency depends exponentially on the molecular weight of an arm [55–57]. A similar trend is found for |η*| at 0.01 rad/s, which increases at t_r = 10 min above the value of vP-HDPE by a factor of 1.8 and 2.4 at T_r = 170 °C and 210 °C, respectively, indicating the build-up of higher molecular weight structures. Due to the terminal double bonds in P-HDPE, as described in literature [34,39–41]. and shown in Fig. 3, star-like branching via crosslinking of those terminal double bonds seems reasonable, which is also supported by the decrease in terminal vinyl content as shown by the IR measurements in Fig. 4A. At 170 °C and longer recycling times, ω_{co} increases again, indicating chain scission and molecular weight reduction, correlating also with the results from SEC. In contrast, at T_r = 210 °C, further crosslinking is happening and after t_r = 240 min, G' and G'' curves even run in parallel to each other at low frequencies with a slope of 0.32, as shown in Figure S3. Those opposing trends at processing temperatures of 170 °C and 210 °C are in general similar to the presented changes in MFI in Fig. 5. The formation of stars via crosslinking of the terminal double bond is also well in line with the changes in the vinyl-index, presented in Fig. 4A and Table S3. In contrast to P-HDPE, recycling ZN-HDPE at both T_r of 170 °C and 210 °C led to relatively small changes of ω_{co} after t_r = 10 and 20 min, but showed an increase of ω_{co} by a factor of 10 and 2.8 after t_r = 30 min, respectively, as shown in

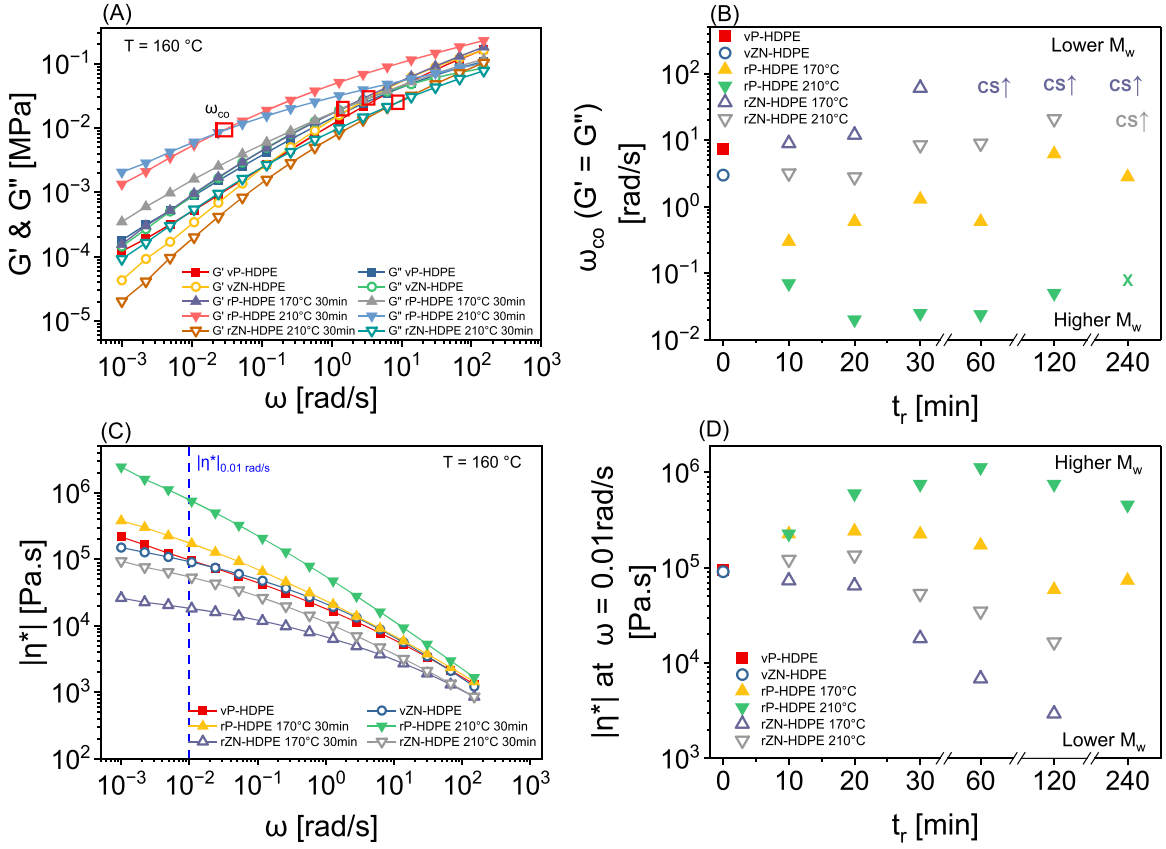

Fig. 6. (A) G' and G'' SAOS data as a function of frequency and at a temperature 160 °C for virgin P—HDPE and ZN-HDPE, rP—HDPE at 30 min and 180 rpm at 170 °C and 210 °C and rZN—HDPE at 30 min and 180 rpm at 210 °C. (B) Crossover frequency of virgin and rP-HDPE and rZN-HDPE as a function of different recycling times. (C) |η*| vs frequency of virgin and rP-HDPE and rZN-HDPE of 30 min at 170 °C and 210 °C. (D) |η*| at 0.01 rad/s of virgin and rP-HDPE and rZN-HDPE as a function of different recycling times.

Fig. 6B Both ω_{co} changes clearly reflect chain scission, thus a M_w reduction. No more crossover point is found for rZN-HDPE after $t_r > 30$ min at $T_r = 170$ °C and after $t_r > 60$ min at $T_r = 210$ °C, as ω_{co} occurs at high frequencies beyond the measurement range due to the drastic M_w decrease. Additionally, $|\eta^*|$ at $\omega = 0.01$ rad/s decreased as a function of t_r and it is given in Fig. 6D, with a drop by a factor of 3.0 and 2.2 after $t_r = 30$ min at $T_r = 170$ °C and 210 °C respectively, which clearly indicates M_w decrease due to chain scission. Those findings also match well the trends observed with the SEC and MFI in Section 3.2 and 3.3. Combining CFC and SAOS rheology indicates that for rZN—HDPE not only chain scission and the formation of linear chains happens, but also the formation of branched structures, which dominate the relaxation process: for a linear polymer, a change in ω_{co} by a factor of 10 would result in a M_w change by a factor of about 2. Since the molecular weight measured with SEC decreases much stronger, is suggests the occurrence of branched structures, with lower hydrodynamic radii, resulting in lower apparent M_w values in SEC.

In overall, rP—HDPE and rZN—HDPE demonstrated different temperature dependent degradation behaviour during mechanical recycling. For rP—HDPE, star-like branching is observed after short $t_r = 10$ min at both temperatures, but at longer t_r chain scission dominates at 170 °C whereas branching to crosslinking occurs at 210 °C. In contrast, rZN—HDPE exhibited at both T_r continuous reduction in $|\eta^*|_{0.01}$ and increasing ω_{co}, indicating chain scission. Furthermore, rZN—HDPE exhibits higher ω_{co} and lower $|\eta^*|_{0.01}$ $T_r = 170$ °C rather than 210 °C, indicating more M_w reduction at 170 °C than at 210 °C, thus degradation is driven for rZN-HDPE more by mechanical shear stress than by temperature.

The conclusions from SAOS rheology regarding changes in topology fit well to the results from DSC and CFC, both indicating the formation of chain irregularities. For rZN—HDPE, changes in M_w captured by rheology and SEC also fit in general well together, whereas it is difficult to draw conclusions for P—HDPE from SEC due to the lack of an absolute molecular mass detection. However, this can be quantified very sensitively by SAOS, highlighting the need and power of combining the two techniques to shed more light on the degradation mechanism of the two HDPE grades polymerized by different catalyst during mechanical recycling.

3.5. Extensional rheology

Whereas DSC and CFC and to some extend SAOS rheology allow to investigate chain irregularities like branching (Fig. 2), to capture "comb-like" LCB and to differentiate from star-like and SCB, extensional rheological measurements are needed. Only long-chain branching causes strain hardening, thus allows to clearly distinguish from SCB or star-like branching. As expected for linear PE, vP-HDPE and vZN-HDPE exhibited negligible strain hardening behaviour, with SHF values between 1.5 and 1.6 and SHF around 1, respectively (Table S4), across all tested strain rates (0.03–3.0 s^{-1}). This response is characteristic of entangled linear polymers with basically no LCB (Figure S5 and Digure S6).

For rP—HDPE recycled at $T_r = 170$ °C and 210 °C, the SHF basically did not change compared to the virgin material until very large $t_r = 240$ min and $t_r = 120$ min, respectively. As stars do not show strain hardening in extensional flow due to topology, these findings support the assumption of the formation of star-like and not comb-like branching from the SAOS experiments. The appearance of SH for $T_r = 170$ °C and $t_r = 240$ min indicates the formation of LCB. For rP-HDPE at $T_r = 210$ °C and large t_r, the occurring relatively weak SH with $SHF_{max} = 3.5$ can be explained by the transition of a star-like topology to crosslinking of the material, as indicated in the SAOS measurements.

Particularly for P-HPDE, the observations from extensional rheology and CFC regarding the changes in CH3/1000 TC are in good agreement: If there is not a (drastic) increase of CH3/1000 TC value above the value of the virgin HPDE, there is also no strain hardening observed.

The molecular degradation during the mechanical recycling in rZN-HDPE left different SH patterns at different T_r. Although the virgin sample showed no strain hardening with a maximum SHF of $SHF_{max} = 1$, as shown in Fig. 7B the SHF_{max} increased continuously with increasing t_r, reaching a $SHF_{max} \approx 5$ after $t_r = 240$ min at $T_r = 170$ °C, but of $SHF_{max} = 11$ at $T_r = 210$ °C, reaching similar SHF_{max} values as most commercial LDPE grades [58–60]. The increase in SHF is due to the development of long-chain branching and clearly indicates more comb-like LCB at $T_r = 210$ °C than at $T_r = 170$ °C.

3.6. Molecular degradation pathways

As shown in Section 3.1 to 3.5 clearly, P-HDPE and ZN—HDPE undergo very different degradation pathways, which differ for P-HDPE and large t_r also clearly between different extrusion temperatures. Due to mechanical stress and heat, C—C bond cleavage and the formation of radicals occur. Those radicals can react further in

(I). recombination with the same or a different radical,
(II). disproportionation or β-chain scission,
(III). the formation of new radicals by e.g., proton abstraction and the formation of a radical within the polymer chain as mid-chain radicals or
(IV). reaction with vinyl groups present in the polymer chains.

Based on the results presented before, we propose the following (dominating) degradation pathways, shown schematically in Fig. 8 and Table S5.

For P-HDPE, star-like branching occurs at short recycling times of $t_r = 10$ min independent of the extrusion temperatures due to crosslinking of the terminal double bonds present in P-HDPE, as indicated by IR spectroscopy, SEC, SAOS rheology and extensional rheology. At longer recycling times, further branching and crosslinking happens at $T_r = 210$ °C, clearly shown by the SAOS data. In contrast, at $T_r = 170$ °C chain scission and branching with a more comb-like long-chain branched topology occurs at long t_r, since ω_{co} from the SAOS data increases with increasing t_r, combined with the occurrence of strain hardening in extensional flow.

The different long-term molecular changes between $T_r = 170$ °C and 210 °C can be explained by more likely C—C bond scission with increasing temperatures, in addition to the more likely further crosslinking of the (remaining) terminal double bonds. The scission of a C—C bond in HDPE leads to the formation of two polymer chains with lower molecular weight and primary radicals. Those polymer chains with a primary radical can abstract a proton from another polymer chain, forming firstly a polymer chain with a mid-chain radical and secondly a proton-terminated lower molecular weight polymer chain. The polymer chain with a mid-chain radical can then react with a polymer chain with another radical. In case of a linear polymer chain with a primary radical, a LCB comb-like structure is formed, which will result in SH. Additionally, comb-like LCB would have a shear thinning effect, matching with the observed SAOS features of again increasing ω_{co} and decreasing $|\eta^*|_{0.01}$ at longer t_r for $T_r = 170$ °C. In contrast, at $T_r = 210$ °C, C—C bond scission is more likely to happen, resulting also in more polymer chains with mid-chain radicals. If overall more mid-chain radicals are present, they are more likely to recombine. If per star-like polymer (as it occurs for P-HDPE after short t_r) in average more than two mid-chain radicals recombine and chemically connect the stars, already a crosslinked network is formed. Here it is very important to note, that only a small portion of crosslinked molecules will fully dominate the resulting bulk dynamics. Thus, it is not necessary that every polymer chain is part of the crosslinked network with the reaction pathway described above, per mid-chain radical also one terminated lower molecular weight polymer chain is produced. Those findings also are in line with the SEC-IR results listed in Table S2, indicating first the decrease of the value of CH3 / 1000 TC during the star formation, and then a final increase with further degradation.

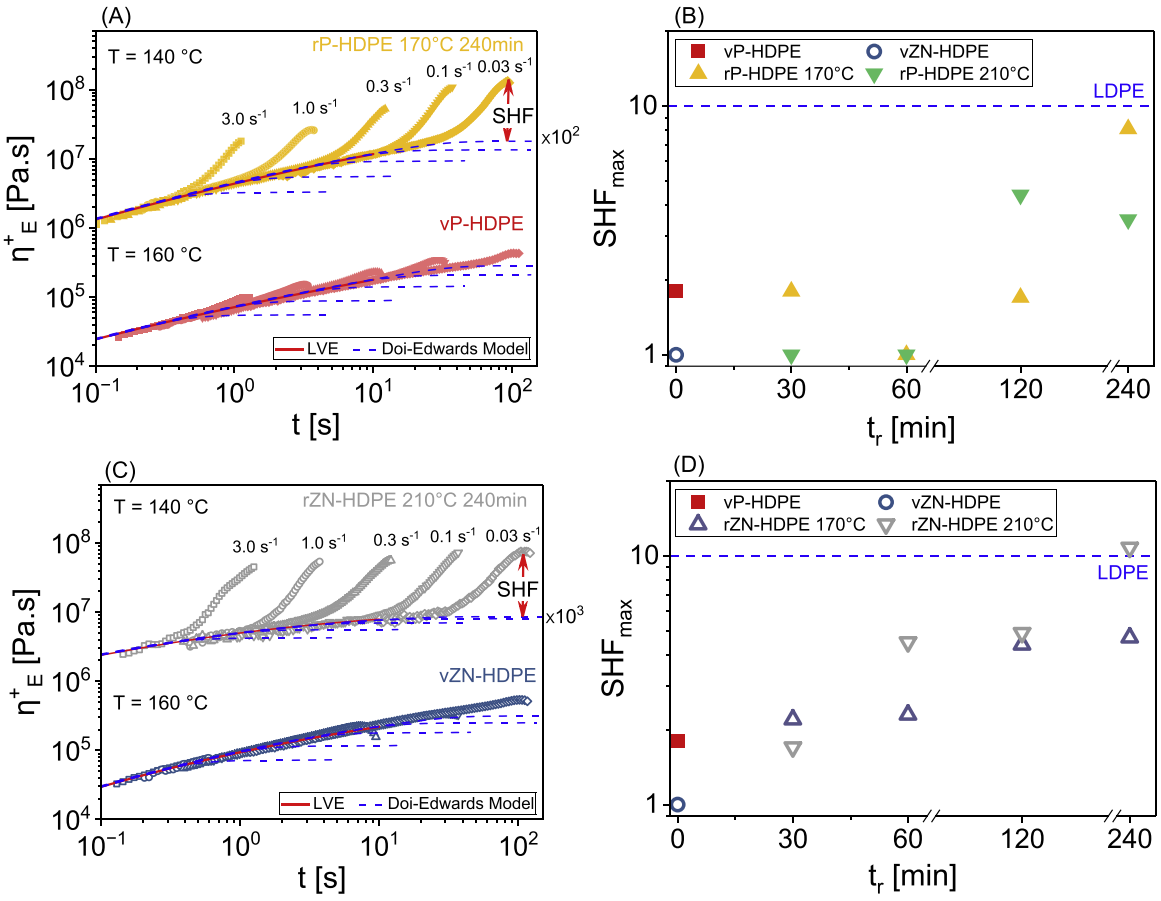

Fig. 7. (A) Transient extensional viscosity as a function of time for vP-HDPE and rP-HDPE processed for 240 min at 180 rpm and 170 °C, and (C) shows extensional viscosity vZN—HDPE and rZN—HDPE processed for 240 min at 180 rpm and 210 °C. The corresponding maximum SHF of rP-HDPE and rZN—HDPE are shown in (B) and (D), respectively.

For ZN—HDPE, chain scission and molecular weight reduction is happening continuously with ongoing recycling time at both extrusion temperatures, as clearly shown by SEC and SAOS rheology. Additionally, DSC and TREF show increased content of branches, with the occurrence of LCB at larger t_r as quantified by the occurrence of SH in extensional flow. Very interestingly, the extent to which those changes happen highly depends on the extrusion temperature: at 210 °C compared to 170 °C, more branching can be found, which is seen consistently throughout DSC, TREF and extensional rheological measurements. From SAOS and SEC measurements, we can conclude more molecular weight reduction at 170 °C than at 210 °C.

While those mechanisms can be derived for the recycling of the neat P- and ZN—HDPE, the mechanism will differ if residual species are available, as it is typically the case for post-consumer waste. The simplest case would be a contamination of ZN—HDPE with P-HDPE, which will clearly impact their degradation pathways.

4. Conclusion

This study provides a polymerization catalyst driven framework for understanding the thermo-mechanical degradation of high-density polyethylene (HDPE) produced via Phillips (P-) and Ziegler-Natta (ZN—HDPE) catalysts during mechanical recycling. Although their chemical similarity, P- and ZN—HDPE differentiate in the number of terminal vinyl groups, as also confirmed by IR spectroscopy. Two blow-moulding virgin P- and ZN—HDPE (vP- and vZN-HDPE) with identical melt flow indices (MFI) were subjected to mechanical recycling using a twin-screw extruder at an extrusion temperature of 170 °C and 210 °C, a screw speed of 180 rpm, and recycling times from 10 to 240 min to simulate mechanical recycling conditions. The HDPE recyclates were characterized with differential scanning calorimetry (DSC), cross-fractionation chromatography (CFC), small angle amplitude oscillatory shear (SAOS) and extensional rheology. The analysis shows distinct and significantly different degradation pathways between P-HDPE and ZN—HDPE. rP-HDPE shows molecular weight increase/star-like branching at short recycling times of 10 min, independent of the recycling temperature, most likely due to crosslinking of the terminal double bonds, correlating with their continuous decrease, quantified by IR spectroscopy. At longer recycling time of >30 min, rP-HDPE shows crosslinking at 210 °C, but chain scission and molecular weight decrease at 170 °C. In contrast, rZN—HDPE shows at both recycling temperatures only chain scission and molecular weight reduction with increasing recycling time, quantified by CFC and SAOS rheology. Interestingly, the molecular weight reduction is more pronounced at 170 °C, whereas at 210 °C more pronounced long-chain branching occurs, resulting in strain hardening in extensional flow. Importantly, the emergence of strain hardening rZN—HDPE particularly under tailored thermal and mechanical histories shows a promising pathway for upcycling it into high-value applications such as films, foams and fibres, where melt strength and strain hardening are critical. These findings highlight for HDPE recycling the importance of polymerization catalyst and the resulting different amount of terminal double bonds for the degradation pathway. Additionally, the here presented framework paves the way to transform waste HDPE into functional materials with enhanced rheological performance. Identifying the polymerization catalyst and/or the amount of terminal bonds before recycling allows to design recycling conditions to obtain high-performances polymer recyclates with tailor-made properties. Therefore, these finding will allow to improve

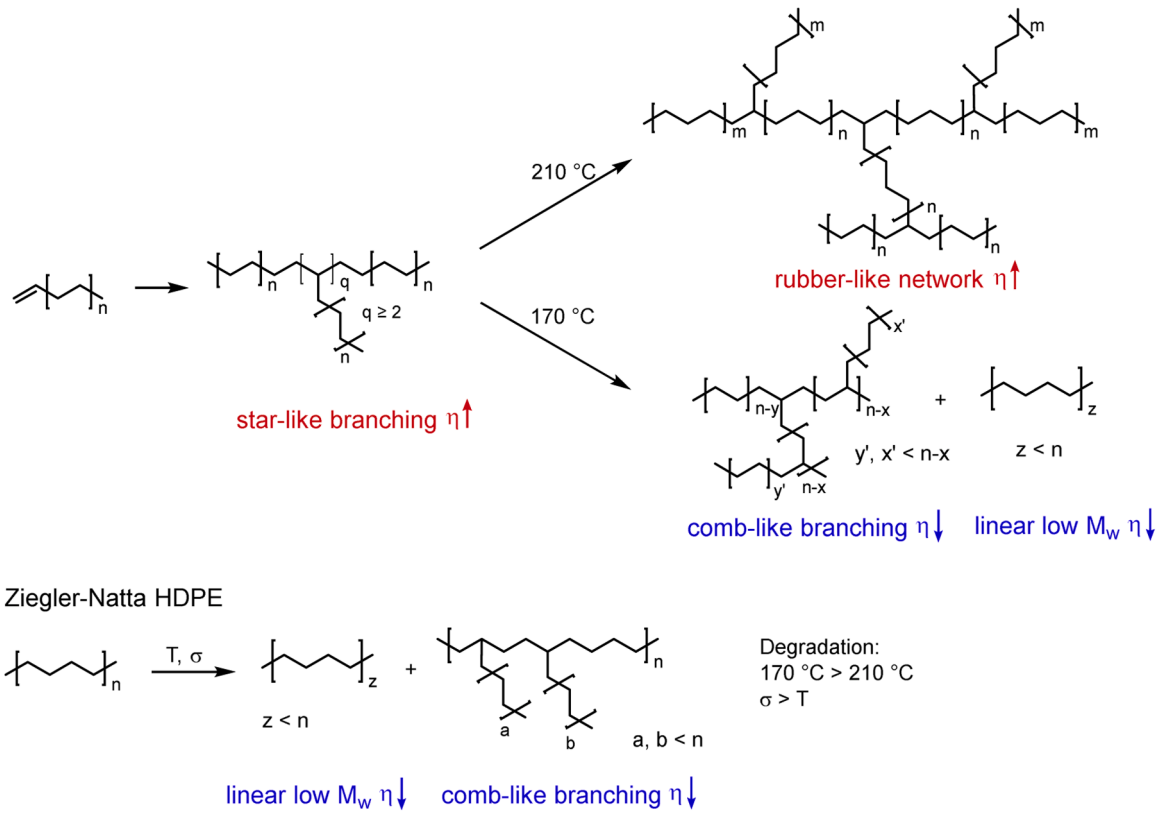

Fig. 8. Schematic drawing of the different degradation pathways and the dominating topologies in P- and ZN—HDPE during mechanical recycling at an extrusion temperature of 170 °C and 210 °C, using the molecular insights from DSC, CFC, SAOS and extensional rheology.

industrial recycling of post-consumer polymer waste and to stop polymer downcycling.

CRediT authorship contribution statement

Alexsandar Arumugam: Writing – original draft, Investigation, Formal analysis. **Jana Zimmermann:** Writing – review & editing, Investigation, Formal analysis. **Thea Weingartz:** Writing – review & editing, Investigation, Formal analysis. **Michael Fischlschweiger:** Writing – review & editing, Validation, Methodology. **Valerian Hirschberg:** Writing – review & editing, Supervision, Project administration, Methodology, Funding acquisition, Conceptualization.

Declaration of competing interest

The authors declare the following financial interests/personal relationships which may be considered as potential competing interests: Michael Fischlschweiger reports financial support was provided by German Research Foundation. If there are other authors, they declare that they have no known competing financial interests or personal relationships that could have appeared to influence the work reported in this paper.

Acknowledgement

The author's thank Mr. Martin Schwedes (ITC, TU Clausthal) for performing the DSC measurements and Mrs. Kai-Anna Keller (IEVB, TU Clausthal) for supporting the CFC analysis, and Dr. Max Schußmann for fruitful discussions regarding the degradation mechanism. Funded by the Deutsche Forschungsgemeinschaft (DFG, German Research Foundation) #453715850.

Supplementary materials

Supplementary material associated with this article can be found, in the online version, at doi:10.1016/j.polymdegradstab.2026.111981.

Data availability

Data will be made available on request.

References

[1] R. Geyer, J.R. Jambeck, K.L. Law, Production, use, and fate of all plastics ever made, Sci. Adv. 3 (2017) e1700782.
[2] P.A. Chen, X. Kang, K. Li, Z. Jian, Tailored synthesis of circular polyolefins, Nat. Sustain. 8 (2025) 422–431.
[3] PlasticsthefastFacts2024-1.
[4] OECD, Policy scenarios for eliminating plastic pollution by 2040, OECD, 2024, https://doi.org/10.1787/76400890-en.
[5] M.D.M.C. López, et al., Assessing changes on poly(ethylene terephthalate) properties after recycling: mechanical recycling in laboratory versus postconsumer recycled material, Mater. Chem. Phys. 147 (2014) 884–894.
[6] M. Häußler, M. Eck, D. Rothauer, S. Mecking, Closed-loop recycling of polyethylene-like materials, Nature 590 (2021) 423–427.
[7] W. Zhang, et al., Highly reactive cyclic carbonates with a fused ring toward functionalizable and recyclable polycarbonates, ACS. Macro Lett. 11 (2022) 173–178.
[8] Q. Xu, H. Yi, X. Gao, J. Shi, D. Yao, Recycling of polyethylene bags into high-strength yarns without using melt processing, Polym. Eng. Sci. 60 (2020) 281–287.
[9] J. Zhang, et al., Effect of mechanical recycling on molecular structure and rheological properties of high-density polyethylene (HDPE), Polymer. (Guildf) 297 (2024) 126866.
[10] J. Zhang, V. Hirschberg, D. Rodrigue, Blending recycled high-density polyethylene HDPE (rHDPE) with Virgin (vHDPE) as an effective approach to improve the mechanical properties, Recycling 8 (2022) 2.
[11] P. Oblak, J. Gonzalez-Gutierrez, B. Zupančič, A. Aulova, I. Emri, Processability and mechanical properties of extensively recycled high density polyethylene, Polym. Degrad. Stab. 114 (2015) 133–145.
[12] A.T.P. Zahavich, B. Latto, E. Takacs, J. Vlachopoulos, The effect of multiple extrusion passes during recycling of high density polyethylene, Adv. Polym. Technol. 16 (1997) 11–24.

[13] T. Schülein, C.K. Georgantopoulos, L. Bolk, V. Herrmann, M. Wilhelm, Thermo-mechanical degradation kinetics of a high-density poly(Ethylene) using a closed-cavity rheometer, J. Appl. Polym. Sci. 142 (2025) e56784.
[14] G. Teteris, Degradation of polyolefines during various recovery processes, Macromol. Symp. 144 (1999) 471–479.
[15] N. Benoit, R. González-Núñez, D. Rodrigue, High density polyethylene degradation followed by closed-loop recycling, Prog. Rubber Plast. Recycl. Technol. 33 (2017) 17–38.
[16] A. Schweighuber, A. Felgel-Farnholz, T. Bögl, J. Fischer, W. Buchberger, Investigations on the influence of multiple extrusion on the degradation of polyolefins, Polym. Degrad. Stab. 192 (2021) 109689.
[17] T. Andersson, B. Stålbom, B. Wesslén, Degradation of polyethylene during extrusion. II. Degradation of low-density polyethylene, linear low-density polyethylene, and high-density polyethylene in film extrusion, J. Appl. Polym. Sci. 91 (2004) 1525–1537.
[18] M.C. Röpert, M.G. Schußmann, M.K. Esfahani, M. Wilhelm, V. Hirschberg, Effect of side chain length in polystyrene POM–POMs on melt rheology and solid mechanical fatigue, Macromolecules. 55 (2022) 5485–5496.
[19] H. Münstedt, Rheological properties and molecular structure of polymer melts, Soft. Matter. 7 (2011) 2273–2283.
[20] A.D. Patel, Z.O.G. Schyns, T.W. Franklin, M.P. Shaver, Defining quality by quantifying degradation in the mechanical recycling of polyethylene, Nat. Commun. 15 (2024) 8733.
[21] J.M. Dealy, D.J. Read, R.G. Larson, Structure and Rheology of Molten Polymers: From Structure to Flow Behavior and Back Again, Carl Hanser Verlag GmbH & Co. KG, München, 2018, https://doi.org/10.3139/9781569906125.
[22] H. Münstedt, S. Kurzbeck, J. Stange, Importance of elongational properties of polymer melts for film blowing and thermoforming, Polym. Eng. Sci. 46 (2006) 1190–1195.
[23] D.A. Pai, O.A. Blake, B.R. Hamaker, O.H. Campanella, Importance of extensional rheological properties on fiber-enriched corn extrudates, J. Cereal. Sci. 50 (2009) 227–234.
[24] R. Liao, W. Yu, C. Zhou, Rheological control in foaming polymeric materials: I. Amorphous polymers, Polymer. (Guildf) 51 (2010) 568–580.
[25] J. Cha, H.Y. Song, K. Hyun, J.S. Go, Rheological measurement of the nonlinear viscoelasticity of the ABS polymer and numerical simulation of thermoforming process, Int. J. Adv. Manuf. Technol. 107 (2020) 2449–2464.
[26] M.H. Wagner, V. Hirschberg, Rheology of poly(α-olefin) bottlebrushes: effect of self-dilution by Alkane side chains, Macromolecules. 57 (2024) 2110–2118.
[27] M.F. Herman, S.F. Edwards, A reptation model for polymer dissolution, Macromolecules. 23 (1990) 3662–3671.
[28] A.L. Kholodenko, Reptation theory: geometrical and topological aspects, Macromol. Theory. Simul. 5 (1996) 1031–1064.
[29] V. Hirschberg, et al., Elongational rheology of 2, 3 and 4 polymer stars connected by linear backbone chains, Rheol. Acta 63 (2024) 407–422.
[30] M.G. Schußmann, M. Wilhelm, V. Hirschberg, Predicting maximum strain hardening factor in elongational flow of branched pom-pom polymers from polymer architecture, Nat. Commun. 15 (2024).
[31] V. Hirschberg, S. Lyu, M.G. Schußmann, M. Wilhelm, M.H. Wagner, Modeling elongational viscosity of polystyrene Pom-Pom/linear and Pom-Pom/star blends, Rheol. Acta 62 (2023) 433–445.
[32] S. Liu, et al., Comparison of shear and extensional rheology between entangled star and linear polystyrenes with the same span molecular weight, Polymer. (Guildf) 339 (2025) 129148.
[33] Genz, U. Dynamics of polymer chains.
[34] C. Brown, et al., Mechanism of initiation in the phillips ethylene polymerization catalyst: ethylene activation by Cr(II) and the structure of the resulting active site, ACS. Catal. 7 (2017) 7442–7455.
[35] M.P. McDaniel, A review of the phillips supported chromium catalyst and its commercial use for ethylene polymerization, in: Advances in catalysis, 53, Elsevier, 2010, pp. 123–606.
[36] G.A. Martino, et al., Cr[CH(SiMe3)2]3/SiO2 catalysts for ethene polymerization: the correlation at a molecular level between the chromium loading and the microstructure of the produced polymer, J. Catal. 394 (2021) 131–141.
[37] J.P. Claverie, F. Schaper, Ziegler-natta catalysis: 50 years after the Nobel Prize, MRS Bull 38 (2013) 213–218.
[38] A. Alikhani, S. Hakim, M. Nekoomanesh, Modified preparation of HDPE/clay nanocomposite by in situ polymerization using a metallocene catalyst, Iran. Polym. J. 26 (2017) 721–731.
[39] E. Epacher, C. Kröhnke, B. Pukánszky, Effect of catalyst residues on the chain structure and properties of a phillips type polyethylen, Polym. Eng. Sci. 40 (2000) 1458–1468.
[40] C.A. Cruz, M.M. Monwar, J. Barr, M.P. McDaniel, Identification of the starting group on the first PE chain produced by the phillips catalyst, Macromolecules. 52 (2019) 5750–5760.
[41] W. Xia, B. Liu, Y. Fang, K. Hasebe, M. Terano, Unique polymerization kinetics obtained from simultaneous interaction of phillips Cr(VI)ox/SiO2 catalyst with Al-alkyl cocatalyst and ethylene monomer, J. Mol. Catal. Chem. 256 (2006) 301–308.
[42] B. Wunderlich, G. Czornyj, A study of equilibrium melting of polyethylene, Macromolecules. 10 (1977) 906–913.
[43] M. Doi, S.F. Edwards, Dynamics of concentrated polymer systems. Part 3.—the constitutive equation, J Chem Soc Faraday Trans 74 (1978) 1818–1832, 2.
[44] M. Doi, S.F. Edwards, Dynamics of concentrated polymer systems. Part 4.—rheological properties, J Chem Soc Faraday Trans 75 (1979) 38–54, 2.
[45] L. Poh, E. Narimissa, M.H. Wagner, Winter, H. H. Interactive shear and extensional rheology—25 years of IRIS Software, Rheol. Acta 61 (2022) 259–269.
[46] A.C. Albertsson, S.O. Andersson, S. Karlsson, The mechanism of biodegradation of polyethylene, Polym. Degrad. Stab. 18 (1987) 73–87.
[47] Boborodea, A. & Brookes, A. GPC and TREF, complementary techniques for complete analysis of polyethylene resins GPC and TREF, complementary techniques for complete analysis of polyethylene resins. (2016).
[48] A. Ortin, B. Monrabal, J. Sancho-Tello, Development of an automated cross-fractionation apparatus (TREF-GPC) for a full characterization of the bivariate distribution of polyolefins, Macromol. Symp. 257 (2007) 13–28.
[49] M. Fischlschweiger, N. Aust, E.R. Oberaigner, C. Kock, Mathematical modeling and optimization of run parameters of crystallization analysis fractionation (CRYSTAF), Macromol. Chem. Phys. 211 (2010) 383–392.
[50] L. Wild, C. Blatz, Development of high performance TREF for polyolefin analysis, in: T.C. Chung (Ed.), New Advances in Polyolefins, Springer US, Boston, MA, 1993, pp. 147–157, https://doi.org/10.1007/978-1-4615-2992-7_11.
[51] W.W. Yau, D. Gillespie, New approaches using MW-sensitive detectors in GPC–TREF for polyolefin characterization, Polymer. (Guildf) 42 (21) (2001) 8947–8958.
[52] J.B.P. Soares, A.E. Hamielec, Temperature rising elution fractionation of linear polyolefins, Polymer. (Guildf) 36 (1995) 1639–1654.
[53] Y. Wang, et al., Unexpected stress overshoot in extensional flow of star polymer melts, ACS. Macro Lett. 13 (2024) 812–817.
[54] P.G. De Gennes, Reptation of a polymer chain in the presence of fixed obstacles, J. Chem. Phys. 55 (1971) 572–579.
[55] Q. Huang, et al., Dynamics of star polymers in fast extensional flow and stress relaxation, Macromolecules. 49 (2016) 6694–6699.
[56] L. Gury, M. Gauthier, M. Cloitre, D. Vlassopoulos, Colloidal jamming in multiarm star polymer melts, Macromolecules. 52 (2019) 4617–4623.
[57] L.J. Fetters, A.D. Kiss, D.S. Pearson, G.F. Quack, F.J. Vitus, Rheological behavior of star-shaped polymers, Macromolecules. 26 (1993) 647–654.
[58] M.H. Wagner, M. Yamaguchi, M. Takahashi, Quantitative assessment of strain hardening of low-density polyethylene melts by the molecular stress function model, J. Rheol. 47 (2003) 779–793.
[59] H. Münstedt, Extensional rheology and processing of polymeric materials, Int. Polym. Process. 33 (2018) 594–618.
[60] P. Micic, S.N. Bhattacharya, Rheology of LLDPE, LDPE and LLDPE/LDPE blends and its relevance to the film blowing process, Polym. Int. 49 (2000) 1580–1589.